

Review

Recent advances of malaria parasites detection systems based on mathematical morphology

Andrea Loddo^{1,†,‡} , Cecilia Di Ruberto^{1,‡} and Michel Kocher^{2,‡}

¹ Department of Mathematics and Computer Science, University of Cagliari; andrea.loddo, dirubert@unica.it

² Biomedical Imaging Group, École Polytechnique Fédérale de Lausanne (EPFL); michel.kocher@heig-vd.ch

* Correspondence: andrea.loddo@unica.it; Tel.: +390706758503

† Current address: Via Ospedale 72, 09124, Cagliari, Italy

‡ These authors contributed equally to this work.

Academic Editor: name

Version December 13, 2017 submitted to Sensors

1 Abstract: This paper investigates existing mathematical morphology based techniques applied for
2 performing malaria parasites detection and identification in both Giemsa and Leishman stained blood
3 smears images. Malaria is an epidemic health disease and a rapid, accurate diagnosis is necessary
4 for proper intervention. Generally, pathologists visually examine blood stained slides for malaria
5 diagnosis; this kind of visual inspection is subjective, error-prone and time consuming. In order
6 to cope with such issues, computer-aided methods have been increasingly evolved for abnormal
7 erythrocyte and/or parasites detection, segmentation and semi/fully automated classification. The
8 aim of this paper is to present a review of recent mathematical morphology based methods for malaria
9 parasite detection.

10 Keywords: malaria, red blood cells segmentation, mathematical morphology, medical image analysis

11 1. Introduction

12 Haematology is the branch of medicine concerned with the study, diagnosis, monitoring,
13 treatment, and prevention of diseases related to the blood and blood-forming organs. Haematology
14 studies the blood in health and pathological conditions, firstly to identify the patient's health condition
15 and, secondly, to predict how the bone marrow may have contributed to reach that condition.

16 Thus, haematology studies the relationship between the bone marrow and the systemic circulation.
17 In fact, there are many diseases, disorders, and deficiencies that can affect the number and type of
18 blood cells produced, their function and their lifespan. Usually, only normal, mature or nearly mature
19 cells are released into the bloodstream but certain circumstances can induce the bone marrow to
20 release immature and/or abnormal cells into the circulation. One of the most frequently ordered
21 test to monitor the proportion of the cell components into the blood stream is the Complete Blood
22 Count (CBC), that offers various hematologic data represented by the numbers and types of cells
23 in the peripheral circulation. The cells percentage is compared with the reference ranges in order to
24 determine if the cells are present in their expected percentage, if one cell type is increased, decreased
25 or if immature cells exist. Reference ranges for blood tests are sets of values used to interpret a set of
26 diagnostic test results from blood samples. Since it is difficult to prove that healthy-considered subjects
27 may not have infections, parasitic infection and nutritional deficiency, it is more feasible to talk about
28 reference ranges rather than normal ranges. A reference range is usually defined as the set of values in
29 which 95% of the normal population falls within. It is determined by collecting data from vast numbers
30 of laboratory tests result from a large number of subjects who are assumed to be representative of
31 the population. With automatic counters or the flow cytometry an automated CBC can be performed

32 quickly. However, if the results from an automated cell count indicate the presence of abnormal cells
33 or if there is a reason to suspect that abnormal cells are present, then a blood smear will be collected
34 [1]. A blood smear is often used to categorize and/or identify conditions that affect one or more types
35 of blood cells and to monitor individuals undergoing treatment for these conditions. The results of
36 a blood smear typically include a description of the cells appearance, as well as any abnormalities
37 that may be seen on the slide. The manual analysis of blood smears is tedious, lengthy, repetitive and
38 it suffers from the presence of a non-standard precision because it depends on the operator's skill.
39 The use of image processing techniques can help to analyse, count the cells in human blood and, at
40 the same time, to provide useful and precise information about cells morphology. Peripheral blood
41 smears analysis is a common and economical diagnosis technique by which expert pathologists may
42 obtain health information about the patients. Although this procedure requires highly trained experts,
43 it is error-prone and could be affected by inter-observer variations. Moreover, blood cells images
44 taken from microscope could vary in their illumination and colouration conditions, as shown in fig. 1.
45 Typical blood cells images contain three main components of interest: the platelets (or thrombocytes),
46 the red blood cells (or erythrocytes) and the white blood cells (or leukocytes). It is worth considering
47 that blood cells exist with different shapes, characteristics and colourations, according to their types.
48 Many tests are designed to determine the number of erythrocytes and leukocytes in the blood, together
49 with the volume, sedimentation rate, and haemoglobin concentration of the red blood cells (blood
50 count). In addition, certain tests are used to classify blood according to specific red blood cell antigens,
51 or blood groups. Other tests elucidate the shape and structural details of blood cells and haemoglobin
52 and other blood proteins. Blood can be analysed to determine the activity of various enzymes, or
53 protein catalysts, that either are associated with the blood cells or are found free in the blood plasma.
54 Blood also may be analysed on the basis of properties such as total volume, circulation time, viscosity,
55 clotting time and clotting abnormalities, acidity (pH), levels of oxygen and carbon dioxide, and the
56 clearance rate of various substances. There are special tests based on the presence in the blood of
57 substances characteristic of specific infections, such as the serological tests for syphilis, hepatitis, and
58 human immunodeficiency virus (HIV, the AIDS virus)¹. Among the several available blood tests,
59 the most common are certainly the blood cells counts, e.g., a CBC is a measure of the hematologic
60 parameters of the blood. Included in the CBC is the calculation of the number of red blood cells
61 (red blood cell count) or white blood cells (white blood cell count) in a cubic millimetre (mm^3) of
62 blood, a differential white blood cell count, a haemoglobin assay, a hematocrit, calculations of red
63 cell volume, and a platelet count. The differential white blood cell count includes measurements
64 of the different types of white blood cells that constitute the total white blood cell count: the band
65 neutrophils, segmented neutrophils, lymphocytes, monocytes, eosinophils, and basophils. A specific
66 infection can be suspected on the basis of the type of leukocyte that has an abnormal value [2].

67 Human malaria infection is not strongly related to cells count but it needs different tests in order
68 to be identified. It can only be caused by parasitic protozoans belonging to the Plasmodium type.
69 The parasites are spread to people through the bites of infected female Anopheles mosquitoes, called
70 "malaria vectors". There are five parasite species that cause malaria in humans and two of these
71 species, Plasmodium Falciparum and Plasmodium Vivax, constitute the greatest threat. Plasmodium
72 Ovale, Plasmodium Malariae and Plasmodium Knowlesi are the three remaining species which are
73 less dangerous in human [3], as shown in fig.2. All five species may appear in four different life-cycle
74 stages during the infection phase in peripheral blood: ring, trophozoite, schizont and gametocyte.
75 Some examples are shown in fig.3. The life-cycle-stage of the parasite is defined by its morphology,
76 size and the presence or absence of malarial pigment. The species differ in the changes of infected
77 cell's shape, presence of some characteristic dots and the morphology of the parasite in some of the
78 life-cycle-stages [4].

¹ <https://www.britannica.com/topic/blood-analysis>

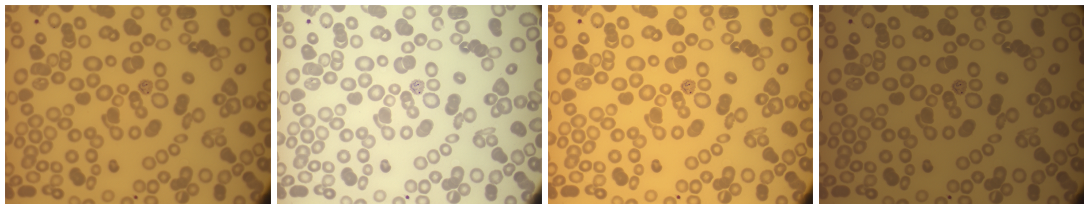


Figure 1. Different illumination conditions generate different images, because of the absence of a standardized acquisition procedure. From left to right: acquisition of the same smear with four microscope's brightness levels.

Courtesy of CHUV, Lausanne.

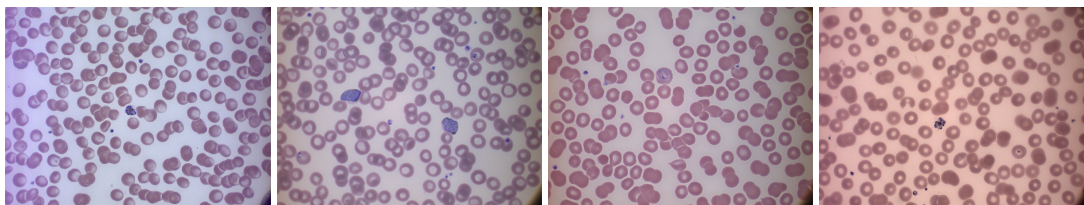


Figure 2. Types of human malaria: from left to right, *P. Falciparum* in its schizont stage, *P. Vivax* in two gametocytes specimens and one ring stage, *P. Ovale* in its ring stage, *P. Malariae* in its schizont stage. Courtesy of CHUV, Lausanne.

79 Computer vision techniques for malaria diagnosis and recognition represent a relatively new
 80 area for early malaria detection and, in general, for medical imaging, able to overcome the problems
 81 related to manual analysis, that is performed by human visual examination of blood smears. The
 82 whole process requires an ability to differentiate between non-parasitic stained components/bodies
 83 (e.g. red blood cells, white blood cells, platelets, and artefacts) and the malarial parasites using
 84 visual information. If the blood sample is diagnosed as positive (i.e. parasites present) an additional
 85 capability of differentiating species and life-stages (i.e. identification) is required to specify the infection.
 86 Numerous methods of automatic malaria diagnosis have been proposed so far, in order to overcome
 87 the issues before mentioned. The aim of this paper is to review and analyse the works of different
 88 researchers who in particular have used mathematical morphology as a powerful tool for computer
 89 aided malaria detection and classification.

90 1.1. Mathematical morphology

91 Mathematical morphology (MM) can be defined as a theory for the analysis of spatial structures.
 92 It is called morphology because it aims at analysing the shape and form of objects. It is mathematical
 93 in the sense that the analysis is based on set theory, integral geometry, and lattice algebra. MM is not
 94 only a theory, but also a very powerful image analysis technique [5]. It was introduced by Matheron
 95 in 1964 as a technique for analysing geometric structure of metallic and geologic samples. It refers
 96 to a branch of non-linear image processing and analysis that concentrates on the geometric structure
 97 within an image. The morphological filter, which can be constructed on the basis of the underlying
 98 morphological operations, are more suitable for shape analysis than the standard linear filters since
 99 the latter sometimes distort the underlying geometric form of the image. Some of the salient points
 100 regarding the morphological approach are as follows [6]:

- 101 • Morphological operations provide for the systematic alteration of the geometric content of an
 102 image while maintaining the stability of the important geometric characteristics.
- 103 • There exists a well-developed morphological algebra that can be employed for representation
 104 and optimization.
- 105 • It is possible to express digital algorithms in terms of a very small class of primitive morphological
 106 operations.

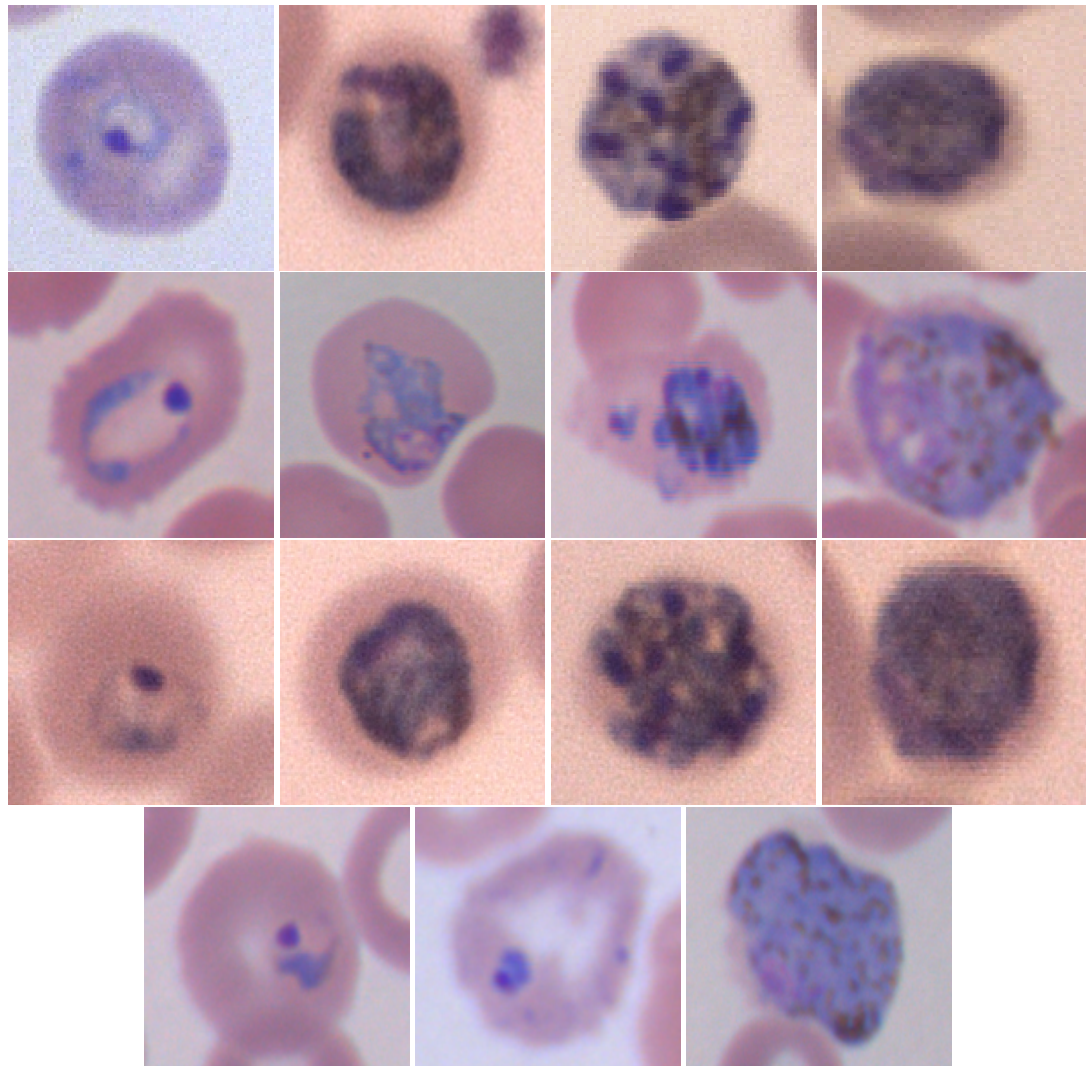


Figure 3. Examples of malaria parasite stages. First row, from left to right: *P.falciparum* ring, trophozoite, schizont, gametocyte; second row, from left to right: *P.ovale* ring, trophozoite, schizont, gametocyte; third row, from left to right: *P.malariae* ring, trophozoite, schizont, gametocyte; last row, from left to right: *P.vivax* ring, developed trophozoite, gametocyte.

Courtesy of CHUV, Lausanne.

- 107 • There exist rigorous representations theorems by means of which one can obtain the expression
108 of morphological filters in terms of the primitive morphological operations.
- 109 Dilation and erosion are the basic morphological processing operations. They are defined in terms of
110 more elementary set operations, but are employed as the basic elements of many algorithms. Both
111 dilation and erosion are produced by the interaction of a set called structuring element (SE) with a set
112 of pixels of interest in the image. The structuring element has both a shape and an origin. From these
113 two basic operators, others have been derived (opening, closing, hit-or-miss). They can be applied to
114 extract image components useful in the representation and descriptions of region shapes, such as area
115 granulometry, boundaries, skeleton, or convex hull. Also, morphological operators can be used for
116 image preprocessing and postprocessing, such as morphological filtering, thinning, and especially for
117 segmentation.

118 2. Scope of this review

119 In this paper we present a review of computer-aided methods oriented to malaria parasites
120 detection and segmentation by mathematical morphology based techniques. Most of the studies were
121 followed Di Ruberto's work [7], which first proposed a system to evaluate parasitaemia in the blood.
122 The system was able to detect the parasites by using an automatic thresholding and morphological
123 operators. A morphological approach to cell segmentation which is more efficient than watershed
124 algorithm [5] was proposed. Finally, the parasites classification was still based on morphological
125 operators. Since then many systems for computer aided diagnosis of malaria have been proposed. Most
126 of them make use of mathematical morphology to process and analyse malaria-infected peripheral
127 blood cells images. The scope of this paper is to review and analyze the recent works of different
128 researchers in the area of malaria parasite recognition using computer vision which benefit from
129 mathematical morphology.

130 The rest of the paper is organised as follows. Section 3 presents a review of the considered
131 works, according to a typical pipeline of a computer-aided image analysis process: preprocessing,
132 segmentation, feature extraction. All the considered works make use of morphological operators in at
133 least one of the phases of image analysis. Section 4 contains an overall discussion about the methods
134 and the conclusions are expressed in section 5.

135 3. Computer aided diagnosis of malaria by using mathematical morphology

136 This section presents a review of some of the main recent studies existing in literature regarding
137 the analysis of malaria infected blood smears using mathematical morphology. A typical approach
138 usually comprises four different image processing and analysis tasks, as follows:

- 139 1. Preprocessing.
- 140 2. Segmentation.
- 141 3. Feature extraction.
- 142 4. Classification.

143 Since morphological techniques have been used in the first three phases, the reviewed works have
144 been divided into the following sub-sections: preprocessing, segmentation and feature extraction.
145 Each sub-section contains description about methods that cope with malaria parasites (MP) stained
146 components analysis, both on thin and thick blood smears, without distinction.

147 Extensive search of articles has been made in PubMed and Google Scholar search engines based
148 on the keywords: "malaria, mathematical morphology, automated malaria diagnosis" up to October
149 2017. The search includes papers published in English and titles and abstracts of potentially relevant
150 studies were selected and presented from the most recent ones. Thereafter, the full texts of these studies
151 were evaluated as per the exclusion criteria.

152 Two main factors are generally considered if we refer to staining techniques: the type of
153 colouration, in which Giemsa and Leishman are the most common, and the thickness of blood slide,
154 which may be thick or thin. The majority of studies have been employed on thin blood smear images
155 (over two-third of the total count) while only a few have used thick blood smear images. Typically,
156 thin smears permit the identification of specific parasitic stage and quantification of malaria parasite;
157 on the other hand, thick smears are better if the target is to perform an initial identification of malaria
158 infection using blood pathology. Some examples are shown in fig. 4. Giemsa stained blood smear is
159 considered in most of the analysed literatures whereas Leishman stain is considered in few studies.
160 It is reported that Leishman stain has bigger sensitivity for parasite detection than Giemsa [8] and
161 is superior for visualization of red and white blood cell morphology [9]. On the contrary, Giemsa
162 stain highlights both malaria parasites and white blood cells and, therefore, it is an additional issue
163 to deal with. Giemsa stain is much costly and also time-taking procedure than Leishman. Moreover,
164 magnification of 100X by using an oil immersion objective is used for capturing microscopic images of
165 thin blood smear for identification of specific parasites and their infected stage.

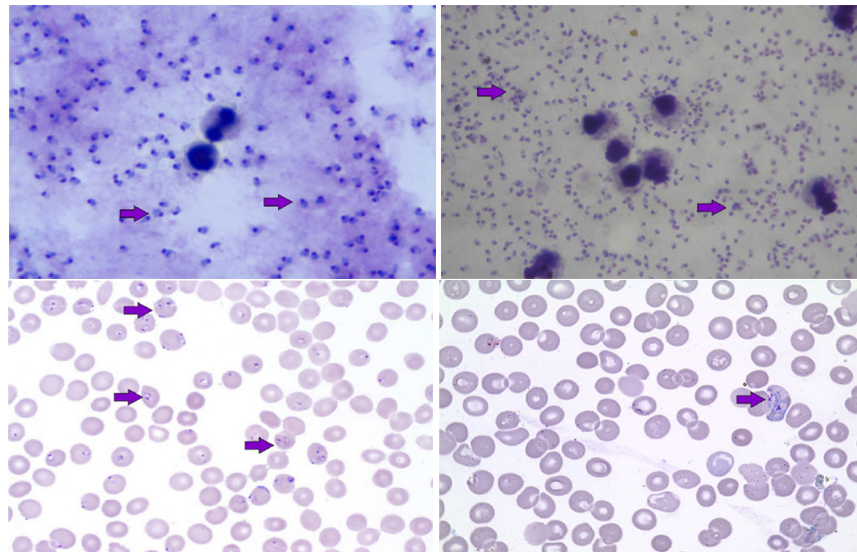


Figure 4. Malaria infected blood smear images. From top left, clockwise: thick smear with Giemsa stain, thick smear with Leishman stain, thin smear with Leishman stain, thick smear with Giemsa stain [10]. Arrows in top images indicate chromatin dots while, in the bottom ones, they show the infected erythrocytes.

166 3.1. Preprocessing

167 In image analysis field, especially when we refer to complex computer-aided pipelines,
 168 preprocessing methods are particularly used in order to improve the image data by suppressing
 169 unwanted noise or enhancing some image features for further processing. It is worth to mention
 170 preprocessing methods because they are an important step regarding image analysis field but, for what
 171 concerns the malaria-affected blood image analysis, in our review we particularly found methods
 172 which operate for illumination correction and noise filtering purposes. Generally speaking, digital
 173 microscopy images can be acquired in different lighting conditions, with several types of acquisition
 174 devices or from blood smears stained with various staining protocols and, consequently, the features
 175 of similar images could differ a lot. Different techniques for illumination correction have been
 176 suggested to reduce such variation, e.g., a lot of authors work with grayscale-converted images
 177 as an illumination correction method. On the other hand, noise filtering aims to remove the noise
 178 introduced by mishandling the slides and/or the camera settings. Morphological operators have
 179 been extensively used as preprocessing for image enhancement in major studies. Erosion and dilation
 180 operations on raw smear images allow discarding undesired patterns and help in the selection of
 181 required cells or regions of interest. Morphological operators are useful for removal of unwanted
 182 objects, holes filling, splitting, thinning and thickening. Different researchers during automated
 183 diagnosis of malaria used morphological operations in preprocessing phase and the most recent are
 184 listed below.

185 In [11] Gonzalez-Betancourt *et al.* proposed a system to determine markers for watershed
 186 segmentation based on the Radon transform and mathematical operators. In the first step of the
 187 process small irrelevant structures and part of the noise are eliminated by a morphological filter, in
 188 order to ensure the preservation of the cells edges. Image smoothing is performed by a morphological
 189 erosion-reconstruction and dilation-reconstruction filter with a disk structuring element of radius
 190 equal to 20 pixels, which is 0.274 times smaller than the average radius of the RBCs. In this way the
 191 influences of the size and the shape of the structures can be separated in the smoothing process. At the
 192 same time the objects which are not eliminated remain unchanged. Also, a morphological closing is
 193 performed with a disk structuring element having radius smaller than half the average of the RBCs
 194 radii, in order to connect the possible (more than one) markers that can appear on a single cell.

In [12] Kareem *et al.* illustrated a morphological approach for blood cell identification and use the image features such as intensity, histogram, relative size and geometry for further analysis. Before the identification of blood cells, the authors propose a novel morphological filtering based on the size of RBC for platelets and/or artifacts elimination. A dilation is performed by a concentric ring structuring element and erosion by a disk-shaped structuring element. The radius of the structuring element depends on the radius of the RBCs, so that all the components smaller than the RBCs can be removed.

The system proposed in [13] by Oliveira *et al.* is based on image processing, artificial intelligence techniques and an adapted face detection algorithm to identify Plasmodium parasites. The latter uses the integral image and haar-like features concepts, and weak classifiers with adaptive boosting learning. The search scope of the learning algorithm is reduced in the preprocessing step by removing the background around blood cells by means of morphological erosions both for training and for testing.

Romero-Rondon *et al.* in [14] presented an algorithm that uses morphological operations, the watershed method, the Hough transform and the clustering method of k-means to detect overlapped RBCs. In the preprocessing stage white blood cells and platelets are removed before the segmentation task. During this step, some noise, the WBC cytoplasm and platelets still remain on the image. Therefore, the small objects are removed using a morphological opening and then the image is dilated with a disk-shaped structuring element.

Reni *et al.* in [15] described a new algorithm for morphological filtering of the blood images as a preprocessing tool for segmentation. Conventional morphological closing on blood images removes the unwanted components but also useful information. On the opposite the proposed method preserves the necessary information of foreground components while removing noise and artefacts.

In the method proposed in [16] by Sheikhhosseini *et al.* the first phase is the stained object extraction which detects candidates objects that can be infected by malaria parasites using intensity and colour. Before detecting the stained objects the method firstly extracts the foreground. Foreground image is a binary image which is produced after applying morphological hole filling on such pixels which have lower intensity value than average intensity value of green layer. After the stained objects extraction process, a series of morphological operations is also employed in order to eliminate small components and complete the final stained objects.

An edge-based segmentation of erythrocytes infected with malaria parasites using microscopic images is proposed by Somasekar *et al.* in [17]. A fuzzy C-means clustering is applied to extract infected erythrocytes, which is further processed for the final segmentation. A morphological erosion is used to erase some small noises and spots before the segmentation and holes inside the infected erythrocytes are filled using a morphological hole filling operation for the final segmentation.

In [18] Tek *et al.* presented a complete framework to detect and identify malaria parasites in images of Giemsa stained thin blood film specimens. Also, the system is able to identify the infecting species and life-cycle stages. The preprocessing step of the proposed method is applied to reduce the variations in the observed size, intensity, and colour of the cells and stained objects before the detection and classification steps. The aim is to correct the non-uniform illumination in the images. The estimation is based on a morphological closing operation using a sufficiently large structuring element. The sufficiently large size for an input image is determined automatically with respect to its average cell size computed from the area granulometry distribution.

237 3.2. Segmentation of RBCs and parasites

Segmentation is a key step in image analysis because it permits the identification and separation of the regions that compose an image, according to certain criteria of homogeneity and separation. Its main target is to divide the image into parts that have a strong correlation with objects or areas of the real world contained in the image. The commonly used segmentation methods essentially operate considering characteristics such as the brightness value, colour and reflection of the individual pixels, identifying groups of pixels that correspond to spatially connected regions. As for many problems of

244 image processing, there is no standard solution valid in general, so different segmentation techniques
245 can be applied, according to the characteristics of the images to process and of the objects to segment.
246 Medical images segmentation is typically performed using two main strategies: the first level aims to
247 separate whole cells or tissues from the background and the second one aims to separate the tissue
248 structure in different regions or the cell in their components, as the nucleus from the cytoplasm or
249 intracellular parasites. The latter case is commonly used in applications in which the cell class depends
250 on the morphological characteristics of its components.

251 Several other authors attempted to use thresholding combined with morphological operation as
252 segmentation method in their computer-aided systems and they are described as follows.

253 Arco *et al.* in [19] worked on thick blood films and proposed a method that uses an adaptive
254 thresholding based scheme, which also allows an effective classification of pixels. This means that the
255 election of whether a pixel belongs to the background or to the signal (parasites and white blood cells)
256 is only established by the pixels around it, that is its neighbourhood. Then, morphological methods
257 are applied to evaluate the area of connected components, labelling those belonging to parasites and
258 counting their number.

259 Anggraini *et al.* [20] proposed a method for separating blood cells, parasites and other components
260 from background in a microscopic field of a thin blood smear. They applied several global thresholding
261 methods and visually compared the results to qualitatively determine which technique yields the best
262 result. The binary image was then subjected to hole filling morphological operator and applied as
263 marker to label blood cells. From each identified cell (RBC and WBC), constituents of the parasite
264 (nucleus and cytoplasm) were extracted using multiple threshold.

265 Dave *et al.* in [21] performed image segmentation using histogram based adaptive thresholding
266 followed by mathematical morphological operations (erosion and dilation). The detection of infected
267 RBCs is based on a unsupervised learning technique.

268 The proposed automated method in [22] by Elter *et al.* for parasite detection and identification
269 worked on thin blood film acquired with Giemsa stain. The authors found that the G and B channels of
270 the RGB colour are very good features to identify objects containing chromatin in Giemsa stained blood
271 films, being not only considered highly discriminative but also almost independent of differences in
272 illumination and staining intensity. They transformed the colour input image into a monochrome
273 image $I(x,y)$, that highlights objects containing chromatin: $I(x,y) = \arctan \frac{I_{green}(x,y)}{I_{blue}(x,y)}$. In this work,
274 mathematical morphology has been used with a black top-hat operator to separate MP from both
275 leukocytes and platelets, with a non-flat paraboloid structuring element of radius of 9 and a slope of 1
276 pixel. It should be taken into account that these fixed parameters might not be suitable for images with
277 different pixel resolutions. The black top-hat operator is followed by a thresholding operation with
278 a fixed threshold, which according to the authors is reliable given the independence of the G and B
279 channels with regard to illumination and staining intensity. However, the authors do not define the
280 value of this fixed threshold on the publication.

281 In [23] Ghosh *et al.* used divergence based threshold selection in order to segment P.vivax parasites
282 from Leishman-stained thin blood films. This method is based on Cauchy membership function [24]
283 and is applied to the C channel of CMYK colour space. Morphological operators of opening and
284 closing have been used for artefacts removal.

285 Kareem *et al.* in [25] used the Annular Ring Ratio transform method. Before applying it, a pre
286 processing phase for removing platelets, parasites and other artefacts in the image has been performed.
287 In the proposed method, the image after being converted to grayscale undergoes a morphological
288 opening similar to closing. Unlike conventional closing (dilation followed by erosion) which uses the
289 same structuring element, two different structuring elements are used, a concentric ring for dilation
290 and a disk for erosion. The inner and outer diameter of the dilation ring is set to 35% and 70% of
291 RBCs size, respectively and the erosion disk has the same diameter. Therefore, considering that fixed
292 manually defined parameters are used for this strategy, the results may substantially differ depending

293 on the image resolution. This approach results in locating only the stained components in the image
294 instead of all the cells and hence will not only speed up the operation but reduces the complexity.

295 Mushabe *et al.* [26] used morphological and statistical classification to detect malaria in blood
296 smears by identifying and counting red blood cells and Plasmodium parasites. Morphological
297 operations and histogram-based thresholding are used to extract RBCs and boundary curvature
298 calculations and Delaunay triangulation are used for splitting clumped RBCs. They worked on
299 Giemsa-stained thin blood smears.

300 In [27] Ross *et al.* proposed a method which provides a positive or negative diagnosis of malaria
301 and differentiates parasites by species. The segmentation step relies on a thresholding strategy which
302 aims to identify and segment potential parasites and erythrocytes from the image background after a
303 six steps threshold selection. Mathematical morphology has been used for parasite size estimation,
304 erythrocytes reconstruction and cells bigger than erythrocytes removal.

305 Savkare *et al.* [28] worked on thin blood films with Giemsa staining and used global threshold
306 and Otsu threshold [29] on grayscale enhanced image (green channel) for separating foreground from
307 background. Hole filling has been performed on identified cells and morphological operators have
308 been used to identify overlapping cells. Then, watershed transform has been applied for separating
309 overlapped cells.

310 Also in the method proposed in [30] by Somasekar *et al.* the segmentation of the infected parasites
311 is based on thresholding. The segmentation is achieved in two stages by maximizing between-class
312 variance of an original image and consequently by an iterative threshold selection from a stage-one
313 threshold image with suitable stopping criteria. The segmented results are post processed to improve
314 the accuracy of the detection of malaria parasites by morphological operators (erosion and closing).

315 On the other hand, a lot of works have been realized by means of mathematical morphology
316 and/or granulometry in the segmentation stages, even in combination with thresholding strategies.
317 They are briefly analysed underneath.

318 Airwhar *et al.* [31] based their approach on thresholding and granulometry. The histogram of
319 the complemented, green component has been used and it is said to be a bimodal distribution in
320 all the considered images. Then, both local and global thresholds are used, and the union of the
321 two binary images is chosen as the parasite marker image. A morphological opening filter, using a
322 disk-shaped SE with radius equal to the mean erythrocyte radius less the standard deviation, is applied
323 to the grayscale morphologically filtered green component of the image to remove any objects smaller
324 than an erythrocyte. The morphological gradient is then calculated using a diamond-shaped SE with
325 unity length. The segmentation method is applied to each object in the reconstructed binary image of
326 erythrocytes individually. Those objects that do not exceed the area of a circle with radius equal to
327 the mean erythrocyte radius plus the standard deviation are regarded as being single cells, and are
328 unmodified. On the other hand, the clumped cells are segmented as follows. First, the intersection of
329 the morphological gradient image and the dilated cell cluster is taken. This image is then transformed
330 to a binary image by thresholding any value greater than zero. A series of morphological operations,
331 namely a closing operation, thinning, and spur removal are then applied to generate a contour of the
332 segmented erythrocytes. The contours are filled, and the segmented mask is again reconstructed with
333 the valid parasite marker image to result in a segmented mask of infected cells.

334 Di Ruberto *et al.* [7] aimed to detect the parasites by means of an automatic thresholding based
335 on a morphological approach applied to cell image segmentation, that is more accurate than the
336 classical watershed-based algorithm. They applied grey scale granulometries based on opening with
337 disk-shaped elements, flat and hemispherical. They used a hemispherical disk-shaped structuring
338 element to enhance the roundness and the compactness of the red cells improving the accuracy of the
339 classical watershed algorithm, while they have used a disk-shaped flat structuring element to separate
340 overlapping cells. These methods make use of the red blood cell structure knowledge, that is not used
341 in existing watershed-based algorithms.

342 Khan *et al.* in [32] presented a novel threshold selection technique used to identify erythrocytes and
343 possible parasites present on microscopic slides that greatly takes benefit of morphological operations,
344 such as granulometry and morphological reconstruction.

345 In [33] Rosado *et al.* proposed a system using supervised classification to assess the presence of
346 malaria parasites and determine the species and life cycle stage in Giemsa-stained thin blood smears.
347 For the RBCs segmentation, they used an adaptive thresholding approach followed by a closing
348 morphological operation with an elliptical structuring element.

349 Soni *et al.* [34] performed segmentation of erythrocytes by using granulometry as well. The
350 size and eccentricity of the erythrocytes are also required for the calculation of some feature values
351 (as these can be indicative of infection). The shape of the objects (circular erythrocytes) is known a
352 priori, but the image must be analysed to determine the size distribution of objects in the image and
353 to find the average eccentricity of erythrocytes present. Gray-scale granulometries based on opening
354 with disk-shaped elements are then used. Non flat disk-shaped structural element are applied to
355 enhance the roundness and compactness of the red blood cells and flat disk-shaped structural element
356 applied to segment overlapping cells. The object to be segmented differs greatly in contrast from the
357 background image. Changes in contrast can be detected by operators that calculate the gradient of an
358 image. The gradient image can be computed and a threshold can be applied to create a binary mask
359 containing the segmented cell. The binary gradient mask is dilated using a vertical structuring element
360 followed by a horizontal structuring element. The cell of interest has been successfully segmented, but
361 it is not the only object that has been found. Any objects that are connected to the border of the image
362 can be removed.

363 In [18] Tek *et al.* the localisation of the parasites is achieved after a foreground and background
364 segmentation step. Firstly, a rough foreground image using morphological area top-hats (using the
365 average cell area value) is extracted. Then, from these rough foreground and background regions two
366 different threshold values are determined and used in morphological double thresholding of the input
367 grey level image to produce a refined binary foreground mask. From the foreground image the stained
368 pixels are detected using again a thresholding approach and finally used as markers to extract the
369 stained objects by morphological area top-hats based on the estimated average area value.

370 In [35] Yunda *et al.* proposed a method for P.vivax parasites detection. The segmentation phase
371 is a combination of border and region detection that allows rejection of the image background and
372 permits identifying each of the objects. Initially, the morphological gradient method is used to enhance
373 the borders of previously found objects. This is followed by a threshold detection stage using the
374 K-Median method. Furthermore, Laplacian operator was used to discriminate the pixels that are
375 interior or exterior in relation to the regions of the images and then erosion operation followed by two
376 dilations were applied to delete the pixels which did not make part of any object. In the end, Absence
377 of Gradients and Nernstian Equilibrium Stripping (AGNES) and K-Median techniques were applied
378 to assign the remaining number of pixels to each region, using the image regions previously identified
379 as objects and background as the starting point.

380 Several authors used marker controlled watershed [5] with morphological approach, as following
381 described.

382 Das *et al.* in [36], [37], [38], [10] segmented erythrocytes as aforesaid and then morphological
383 operators are used to eliminate unwanted cells like leukocytes and platelets. To conclude, overlapping
384 erythrocytes are segmented by using marker controlled watershed segmentation technique.

385 In the paper [39] Devi *et al.* proposed a computer assisted system for quantification of erythrocytes
386 in microscopic images of thin blood smears. The performance of the system in classifying the isolated
387 and clump erythrocytes by geometric features is evaluated for the different classifiers. The clump
388 erythrocytes are segmented using marker controlled watershed with h-minima as internal marker.

389 In [40] Dey *et al.* presented an automatic system for segmenting platelets, useful for identifying
390 disease as malaria, using a color based segmentation and mathematical morphology (opening
391 operations with a disk element of radius 2).

392 In the study presented in [41] by Diaz *et al.* for quantification and classification of erythrocytes
393 in stained thin blood films infected with Plasmodium falciparum, the authors used connected
394 morphological operators in the segmentation step. The RBCs are detected as follows: firstly, a pixel
395 classification allowed to label each image pixel as either background or foreground, based on its color
396 features. Afterward, an inclusion-tree structure is used to represent the hierarchical object relations
397 between background and foreground so that a filtering process allows to remove irrelevant structures
398 such as artifacts generated at the staining or digitization processes.

399 Khan *et al.* [32], among other experimentations, used it in order to try to separate overlapping
400 cells because, according to their statements, watershed transform can separate touching cells but it is
401 not sufficient for overlapping cells.

402 In the algorithm described by Romero-Rondon *et al.* in [14] the detection of overlapped RBCs is
403 still based on marker-controlled watershed transform. To define the suitable markers in watershed
404 transform they used three different approaches, based on a morphological erosion operation, on Hough
405 transform and on clustering method of K-means.

406 Savkare *et al.* in [42] segmented cells using K-mean clustering and global threshold. Overlapping
407 cells are separated using Sobel edge detector and watershed transform. Watershed transform is applied
408 on each cluster separately. Over-segmentation is minimized by series of morphological operations,
409 like erosion and dilation utilizing disk-shaped structuring elements.

410 In [43] an approach to detect red blood cells with consecutive classification into parasite infected
411 and normal cells for further estimation of parasitemia is proposed. For separation of overlapping cells
412 watershed transform is applied on distance transform of binary mask of cells having larger area.

413 In [44] Špringl performed red blood cell segmentation by using marker-controlled watershed
414 transformation based on the image gradient. Markers are computed as a combination of the binary
415 mask of the red blood cells and centres of the cells which are computed using a similar algorithm that
416 was utilized for the evaluation of the average cell radius. The binary mask is obtained by thresholding
417 the grey-scale image with an automatically estimated threshold using Otsu method [29].

418 In [45] Sulistyawati *et al.* combined morphological operations (erosion, dilation, opening and
419 closing) and blob analysis to segment and identify malaria parasites with a high degree of accuracy.

420 Tek *et al.* in [46] proposed a classifier-based method, for the segmentation stage, which relies
421 on a Bayesian pixel classifier to distinguish among stained and non-stained pixels. In particular,
422 they used a non-parametric method based on histograms in order to produce the probability density
423 functions of stained and non-stained classes. Stained pixels can belong to other components such
424 as WBCs, platelets or artefacts, in addition to the parasites and so the detection procedure requires
425 a further classification to distinguish among parasite and non-parasite pixels. However, the stained
426 pixels have to be represented as connected sets, representing stained objects, to extract features for the
427 classifier. Furthermore, top-hat extraction and infinite reconstruction were applied to find the regions
428 that include the objects.

429 To conclude, many systems for computer aided diagnosis of malaria disease made use of
430 mathematical operations in order to smoothen the boundary of the regions obtained from the
431 segmentation process.

432 3.3. Feature extraction

433 Feature extraction has the target of reducing the computational complexity of the subsequent
434 process and facilitating a reliable and accurate recognition for unknown novel data, considering
435 that the input data to an algorithm could be too large to be processed and it could be redundant
436 (e.g. repetitiveness of pixels patterns in an image). Moreover, the in-depth understanding of the
437 domain-specific knowledge gained by human experts on the problem being addressed can be of
438 extreme importance for the design of a reliable and effective feature extraction engine [47]. It starts
439 from determining a subset of the initial features and this procedure is called feature selection. The
440 selected features are expected to contain the relevant information from the input data, so that the

441 desired task can be performed by using this reduced representation instead of the complete initial
442 data. Malaria parasite infection causes micro structural changes in erythrocytes. The microscopic
443 features of the RBCs are usually specific to morphology, intensity and texture. They may also represent
444 the differences that occur among healthy and unhealthy cells. Most of the studies have reported
445 both textural and geometric features for describing malaria infection stages [10]. Generally speaking,
446 features may be distinguished according to the following characteristics: morphological features and
447 textural and intensity features.

448 It is a well known mathematical morphology approach to compute a size distribution of grains in binary
449 images, using a series of morphological opening operations. It is the basis for the characterization
450 of the concept of size. Some authors used area granulometry for preprocessing purposes in malaria
451 characterization [18] even though it is certainly effective for extracting cells size features information
452 [46],[48],[44]. In [18] local area granulometry combined with colour histogram are used as features.
453 The area granulometry feature is calculated locally on the binary mask of the stained objects, for the
454 RGB channels and then concatenated. Morphological features are also used in [36] (opening, closing)
455 and in [7] (skeleton) to classify parasites.

456 4. Discussions

457 In the review we have only considered the methods which employed mathematical morphology
458 in at least one step of the pipelines and it has been structured by considering the following information:
459 preprocessing, segmentation, features extraction. Most of the studies are based on *P. vivax* and/or
460 *P. falciparum* characterization. With regards to the showed approaches and related results, it is clear
461 that malaria parasites detection and segmentation techniques in microscopic images needs further
462 experiments and improvements. In general, the analysed works have been tested with a limited
463 number of images and the datasets are not publicly available; therefore, a comparison between
464 different approaches is very difficult. Despite promising results reported during the past years,
465 the great majority of the computer-aided methods found on the literature for malaria diagnosis are
466 based on images acquired under well controlled conditions and with proper microscopic equipment.
467 However, one should take into account that 80% of malaria cases occur in Africa, where this type of
468 equipment is scarce or even nonexistent in common healthcare facilities [33]. Moreover, this review
469 showed that *P. falciparum* is the most analysed if we refer to segmentation and detection, considering
470 that it is the most widespread among malaria parasite types. The majority of the works used thin
471 blood smear. It is typically used for identification of malaria infected stages, types of parasitic infection
472 and percentage of parasitemia, while thick blood smear is used for identification and quantification of
473 malaria parasite count against leukocyte count per microliter blood.

474 Preprocessing phase is typically taken on with filters and the most used in the analysed works is
475 certainly the median filter which permits to preserve sharp edges. Apart from the classic histogram
476 equalization and contrast stretching techniques, other filters have been employed, e.g., geometric mean
477 filter to remove Gaussian noise preserving edges, Laplacian filter, in order to find edges, and so on.
478 Median filter has been found to be effective for reducing impulse noises from the microscopic images,
479 even though recent studies have shown that geometric mean filter provides better performance than
480 the median filter [37], [10]. However, morphological operators have been greatly used with successful
481 performances, imposing themselves as powerful alternatives to more common and used techniques
482 for image enhancement and noise filtering ([7], [11], [25], [12], [48], [26], [13], [15], [14], [27] [16], [17],
483 [44], [18]).

484 Malaria parasites may be discriminated according to two different strategies: by segmenting the
485 whole erythrocyte from the blood smear image on the basis of which malaria infection is detected,
486 otherwise by segmenting chromatin dot or parasite infection region for characterizing parasite infection
487 stages based on some extracted target features. In general, thresholding-based approach is still widely
488 used for segmentation purposes. In particular, a lot of authors affirm that Otsu thresholding suffers
489 from limitations when textural variation is high, while histogram thresholding can not deal sufficiently

490 good in identifying valley regions in case of unimodal histograms. However, such a simple and fast
491 approach can greatly benefit from mathematical morphology as recent studies demonstrate ([31], [20],
492 [19], [7], [22], [23], [25], [26], [33], [27], [28], [42], [30], [18]).

493 Another greatly used segmentation approach is clearly the watershed transform. The classic
494 watershed approach is reported to produce over segmentation results [28], whereas the marker
495 controlled approach does not suffer from this issue and it is reported to be very effective for overlapping
496 cells segmentation even though some authors affirm that it may fail to segment highly overlapped
497 cells ([36], [37], [38], [10], [39], [32], [14], [42], [43], [44]).

498 Other authors ([31], [7], [32], [26], [27], [34], [18]) employed granulometry and stated that it is
499 very effective to segment cells with regular size.

500 The analysed works performed classification phase for different purposes. The majority of them
501 aimed to distinguish among two classes only, malaria infected and noninfected RBCs, or to detect and
502 count parasites in a malaria blood image ([20], [19], [36], [21], [10], [7], [22], [23], [12], [8], [48], [26],
503 [13], [28], [43], [4], [17], [30], [34], [45], [46]).

504 More complex classification strategies aimed to classify parasites into different classes, i.e. different
505 human parasites species ([31], [37], [38], [32], [18]), and/or different parasites life stages ([20], [37], [38],
506 [7], [41], [18]).

507 A summary of analysed methods is shown in Table 1.

508 5. Conclusions

509 This work reviewed several computational microscopic imaging techniques oriented to
510 mathematical morphology approach, proposed in literature for malaria parasites detection and
511 segmentation in blood smear microscopic images.

512 The computer vision methodologies reported in the literature are based on light microscopic
513 images of human peripheral blood smears for computer-aided detection of malaria parasites and their
514 different life stages. Image preprocessing, segmentation of erythrocytes and parasites, malaria parasite
515 feature extraction, malaria detection techniques have been discussed here.

516 It is worth noticing that cells colours and the colour contrast between cells and background can
517 vary so often according to the different, existing staining techniques, thickness of smear, microscope
518 illumination and microscope's image acquisition procedure, as shown in fig. 1. A standardization
519 of the procedure should be really useful to avoid superfluous differences in similar images' features
520 and to have fair comparisons among the several proposed methods. The main efforts towards the
521 realization of a fully automatic blood cells segmentation and classification system cannot leave this
522 aspect out.

523 Mathematical morphology techniques have been widely used for image processing purposes.
524 Among the application fields, it has been applied for fingerprint feature extraction, recognition of
525 handwritten digits, license plate detection, border extraction, denoising using morphological filters,
526 text extraction and detection of imperfection in printed circuit boards [49]. Apart from this kind
527 of fields, mathematical morphology has been employed successfully in biomedical image analysis,
528 especially in preprocessing and segmentation techniques.

529 Morphological cell analysis is used to face off abnormality identification and classification, early
530 cancer detection. It has been integrated in new methods for biomedical applications, such as automatic
531 segmentation and analysis of histological tumour sections, boundary detection of cervical cell nuclei
532 considering overlapping and clustering, the granules segmentation and spatial distribution analysis,
533 morphological characteristics analysis of specific biomedical cells, understanding the chemotactic
534 response and drug influences, or identifying cell morphogenesis in different cell cycle progression.
535 Morphological feature quantification for grading cancerous or precancerous cells is especially widely
536 researched in the literature, such as nuclei segmentation based on marker-controlled watershed
537 transform and snake model for hepatocellular carcinoma feature extraction and classification, which
538 is important for prognosis and treatment planning, nuclei feature quantification for cancer cell cycle

539 analysis, and using feature extraction including image morphological analysis, wavelet analysis, and
540 texture analysis for automated classification of renal cell [50].

541 Moreover, non-linear filtering has become increasingly important in many image processing
542 applications. Initially, the attraction to non-linear filters was mostly limited to the impulse-removing
543 and edge-preserving qualities of the median filter. However, as the number and sophistication of
544 non-linear filters have increased, so has the variety of applications for these filters. The shape-based
545 methods of mathematical morphology, in particular, are now used in a wide variety of medical
546 applications, including electrocardiography, ultrasound imaging, radiology, and histological image
547 analysis [51].

548 Furthermore, microscopic image analysis and, in particular, malaria detection and classification
549 can greatly benefit from the use of mathematical morphology. The interest in this approach to image
550 processing ad analysis is proved by the increasing number of works proposing methods for malaria
551 image analysis based on mathematical morphology techniques.

552 In the end, it is worth considering that the development of new mobility-aware microscopic
553 devices (and ideally low cost) is an area that can greatly improve the chances of the successful
554 deployment of computer vision CAD solutions for malaria diagnosis in the field. The mobile phone is
555 currently Africa's most important digital technology, and is boosting African health as it emerges as a
556 platform for diagnosis and treatment. Considering the recent significant improvements of the new
557 generation of mobile devices in terms of image acquisition and processing power, if a reliable automatic
558 diagnostic performance is ensured through the usage of those devices, one would dramatically reduce
559 the effort in the exhaustive and time consuming activity of microscopic examination. Moreover, the
560 lack of highly trained microscopists on malaria diagnosis in rural areas could then be complemented
561 by a significantly less specialized technician that knows how to operate the system and prepare blood
562 smears. The usage of mobile devices in the system architecture can also bring significant improvements
563 in terms of portability and data transmission, like the systems proposed by [13] and [33]. Finally,
564 malaria diagnosis might be just one element of a suite of diagnostic software tests running on this type
565 of system. Several other tests could simultaneously be carried out using the same images, for instance
566 cell counting or detection of other hemoparasites, like microfilaria or trypanosoma [52].

Authors	Preprocessing	Segmentation	Classification	Performance
Ahirwar <i>et al.</i> , 2012	-	thresholding + granulometry, opening, morphological gradient, dilation, closing, thinning, spur removal	five (<i>P.falciparum</i> , <i>P.vivax</i> , <i>P.ovale</i> , <i>P.malariae</i> infected, and noninfected)	-
Anggraini <i>et al.</i> , 2011	-	thresholding + hole filling	two (<i>P.falciparum</i> infected and noninfected) + two life-cycle-stages	SE=93% SP=99%
Arco <i>et al.</i> , 2014	-	adaptive thresholding + hole filling, closing, regional minima	two (infected and noninfected)	Acc=96.46%
Das <i>et al.</i> , 2011	-	marker controlled watershed + opening, closing	two (infected and noninfected)	Acc=88.77%

Das <i>et al.</i> , 2013	-	marker controlled watershed	three (<i>P.falciparum</i> , <i>P.vivax</i> infected and noninfected) + three life-cycle-stages per species	Acc=84%
Das <i>et al.</i> , 2014	-	marker controlled watershed	three (<i>P.falciparum</i> , <i>P.vivax</i> infected and noninfected) + three life-cycle-stages per species	SE=99.72% SP=84.39%
Dave <i>et al.</i> , 2017	-	adaptive thresholding + erosion, dilation	two (infected and noninfected)	Acc=97.83% thin films, Acc=89.88% thick films
Devi <i>et al.</i> , 2017	-	marker controlled watershed	two (infected and noninfected)	Acc=98.02%
Diaz <i>et al.</i> , 2009	-	inclusion tree	two (<i>P.falciparum</i> infected and noninfected) + three life-cycle-stages	SE=94% SP=99.7% for detection, SE=78.8% SP=91.2% for life-stages
Di Ruberto <i>et al.</i> , 2002	area closing, opening	thresholding + granulometry, watershed transform + skeleton	two (<i>P.falciparum</i> infected and noninfected) + three life-cycle-stages	-
Elter <i>et al.</i> , 2011	-	thresholding + black top-hat, dilation	two (infected and noninfected)	SE=97%
Gonzalez-Betancourt <i>et al.</i> , 2016	morphological filter, erosion-reconstruction, dilation-reconstruction, closing	watershed transform	-	-
Ghosh <i>et al.</i> , 2011	-	thresholding + opening, closing	two (<i>P.vivax</i> infected and noninfected)	-
Kareem <i>et al.</i> , 2011, 2012	dilation, erosion	-	two (infected and noninfected)	Acc=88% SE=90% SP=86%
Khan <i>et al.</i> , 2011	area closing	thresholding + granulometry, opening, morphological reconstruction, gradient, dilation	five (<i>P.falciparum</i> , <i>P.vivax</i> , <i>P.ovale</i> , <i>P.malariae</i> infected, and noninfected)	Acc=81% SE=85.5%
Malihi <i>et al.</i> , 2013	closing	area granulometry	two (infected and noninfected)	Acc=91% SE=80% SP=95.5%
Mushabe <i>et al.</i> , 2013	closing	thresholding + granulometry, dilation, erosion	two (infected and noninfected)	SE=98.5 SP=97.2%
Oliveira <i>et al.</i> , 2017	erosion	-	two (infected and noninfected)	Acc=91%

Reni <i>et al.</i> , 2015	new morphological filtering	-	-	-
Romero-Rondon <i>et al.</i> , 2016	dilation, opening	marker controlled watershed, erosion	-	-
Rosado <i>et al.</i> , 2017	-	adaptive thresholding + closing	four (<i>P.falciparum</i> , <i>P.ovale</i> , <i>P.malariae</i> infected, and noninfected) + three life-cycle-stages for species	SE=73.9-96.2% SP=92.6-99.3%
Ross <i>et al.</i> , 2006	area closing	thresholding + granulometry, opening, reconstruction, morphological gradient, closing, thinning	five (<i>P.falciparum</i> , <i>P.vivax</i> , <i>P.ovale</i> , <i>P.malariae</i> infected, and noninfected)	SE=85% for detection, Acc=73% for classification
Savkare <i>et al.</i> , 2011a	-	thresholding + hole filling, watershed transform	two (infected and noninfected)	-
Savkare <i>et al.</i> , 2011b	-	thresholding + hole filling, watershed transform	two (infected and noninfected)	SE=93.12% SP=93.17%
Savkare <i>et al.</i> , 2015	-	thresholding + watershed transform, erosion, dilation	two (infected and noninfected)	Acc=95.5%
Sheikhhosseini <i>et al.</i> , 2013	hole filling	thresholding + hole filling, opening	two (infected and noninfected)	Acc=97.25% SE=82.21% SP=98.02%
Somasekar <i>et al.</i> , 2015	erosion	fuzzy C-means clustering + erosion, hole filling	two (infected and noninfected)	SE=98% SP=93.3%
Somasekar <i>et al.</i> , 2017	-	thresholding + erosion, closing, hole filling	two (infected and noninfected)	average DSC=0.8
Soni <i>et al.</i> , 2011	-	thresholding + granulometry, morphological gradient, dilation	five (<i>P.falciparum</i> , <i>P.vivax</i> , <i>P.ovale</i> , <i>P.malariae</i> infected, and noninfected)	SE=98% for detection
Špringl, 2009	closing	thresholding + marker controlled watershed transform, hole filling, dilation, opening, erosion	two (infected and noninfected)	AUC=0.98

Sulistyawati <i>et al.</i> , 2015	-	blob analysis + erosion, dilation, opening, closing, hole filling	two (infected and noninfected)	Acc=99.39%
Tek <i>et al.</i> , 2006	-	top-hat, infinite reconstruction, area granulometry	two (infected and noninfected)	SE=74% SP=98%
Tek <i>et al.</i> , 2010	closing, granulometry	thresholding + granulometry, area top-hat, closing, area granulometry	five (<i>P.falciparum</i> , <i>P.vivax</i> , <i>P.ovale</i> , <i>P.malariae</i> infected, and noninfected) + four life-cycle-stages for species	SE=72% SP=98%
Yunda <i>et al.</i> , 2012	-	thresholding + morphological gradient, erosion, dilation	three (<i>P.falciparum</i> , <i>P.vivax</i> infected, and noninfected) + two life-cycle-stages for <i>P.falciparum</i>	SE=77.19%

Table 1. Summary of analysed methods: morphological operations used in the main phases of analysis, kind of classification and performance measures (Sensitivity, Specificity, Accuracy, if reported).

Acknowledgments: All sources of funding of the study should be disclosed. Please clearly indicate grants that you have received in support of your research work. Clearly state if you received funds for covering the costs to publish in open access.

Conflicts of Interest: The authors declare no conflict of interest.

Abbreviations

The following abbreviations are used in this manuscript:

CBC	Complete Blood Count
WBC	White Blood Cell
RBC	Red Blood Cell
MM	Mathematical Morphology
MP	Malaria Parasite
SE	Structuring Element

575

1. Loddo, A.; Putzu, L.; Di Ruberto, C.; Fenu, G. A Computer-Aided System for Differential Count from Peripheral Blood Cell Images. 2016 12th International Conference on Signal-Image Technology Internet-Based Systems (SITIS), 2016, pp. 112–118.
2. Di Ruberto, C.; Loddo, A.; Putzu, L. A leucocytes count system from blood smear images: Segmentation and counting of white blood cells based on learning by sampling. *Machine Vision and Applications* **2016**, 27, 1151–1160.
3. WHO. Malaria fact sheet December 2016, 2016.
4. Somasekar, J. Computer vision for malaria parasite classification in erythrocytes. *International Journal on Computer Science and Engineering* **2011**, 3, 2251–2256.
5. Soille, P. *Morphological Image Analysis: Principles and Applications*; Springer, 2004; p. 392, [1011.1669].
6. Giardina, C.; Dougherty, E. *Morphological Methods in Image and Signal Processing*; Prentice-Hall, Inc.: Upper Saddle River, NJ, USA, 1988.
7. Di Ruberto, C.; Dempster, A.; Khan, S.; Jarra, B. Analysis of infected blood cell images using morphological operators. *Image and Vision Computing* **2002**, 20, 133 – 146.

- 590 8. Khan, N.; Pervaz, H.; Latif, A.; Musharraf, A.; Saniya. Unsupervised identification of malaria parasites
591 using computer vision. 2014 11th International Joint Conference on Computer Science and Software
592 Engineering (JCSSE), 2014, pp. 263–267.
- 593 9. Sathpathi, S.; Mohanty, A.; Satpathi, P.; Mishra, S.; Behera, P.; Patel, G.; Dondorp, A. Comparing Leishman
594 and Giemsa staining for the assessment of peripheral blood smear preparations in a malaria-endemic
595 region in India. *Malaria Journal* **2014**, *13*, 512.
- 596 10. Das, D.; Mukherjee, R.; Chakraborty, C. Computational microscopic imaging for malaria parasite detection:
597 a systematic review. *Journal of microscopy* **2015**, *260*, 1–19.
- 598 11. Gonzalez-Betancourt, A.; et alt., P.R.R. Automated marker identification using the Radon transform for
599 watershed segmentation. *IET Image Processing* **2016**, *11*, 183–189.
- 600 12. Kareem, S.; Kale, I.; Morling, R. Automated Malaria Parasite Detection in Thin Blood Films:- A Hybrid
601 Illumination and Color Constancy Insensitive, Morphological Approach. Proc. of the 2012 IEEE Asia
602 Pacific Conference on Circuits and Systems (APCCAS), 2012.
- 603 13. Oliveira, A.; Prats, C.; Espasa, M.; et al.. The Malaria System MicroApp: A New, Mobile Device-Based Tool
604 for Malaria Diagnosis. *JMIR Research Protocols* **2017**, *6*, 1–11.
- 605 14. Romero-Rondon, M.; Sanabria-Rosas, L.; Bautista-Rozo, L.; Mendoza-Castellanos, A. Algorithm for
606 detection of overlapped red blood cells in microscopic images of blood smears. *DYNA* **2016**, *83*, 187–194.
- 607 15. Reni, S.; Kale, I.; Morling, R. Analysis of Thin Blood Images for Automated Malaria Diagnosis. Proc. of the
608 5th IEEE International Conference on E-Health and Bioengineering - EHB 2015, 2015.
- 609 16. Sheikhhosseini, M.; Rabbani, H.; Zekri, M.; Talebi, A. Automatic diagnosis of malaria based on complete
610 circle ellipse fitting search algorithm. *Journal of Microscopy* **2013**, *252*, 189–203.
- 611 17. Somasekar, J.; Reddy, B. Segmentation of erythrocytes infected with malaria parasites for the diagnosis
612 using microscopy imaging. *Computers and Electrical Engineering* **2015**, *45*, 336–351.
- 613 18. Tek, F.; Dempster, A.; Kale, I. Parasite detection and identification for automated thin blood film malaria
614 diagnosis. *Computer Vision and Image Understanding* **2010**, *114*, 21 – 32.
- 615 19. Arco, J.; Gorri, J.; Ramirez, J.; Alvarez, I.; Puntonet, C. Digital image analysis for automatic enumeration
616 of malaria parasites using morphological operations. *Expert Systems with Applications* **2014**, *42*, 3041 – 3047.
- 617 20. Anggraini, D.; Nugroho, A.; Pratama, C.; Rozi, I.; Iskandar, A.; Hartono, R. Automated status identification
618 of microscopic images obtained from malaria thin blood smears. Proceedings of the 2011 International
619 Conference on Electrical Engineering and Informatics, 2011, pp. 1–6.
- 620 21. Dave, I.; Upla, K. Computer Aided Diagnosis of Malaria Disease for Thin and Thick Blood Smear
621 Microscopic Images. 2017 4th International Conference on Signal Processing and Integrated Networks
622 (SPIN), 2017, pp. 561–561.
- 623 22. Elter, M.; Haßlmeyer, E.; Zerfaß, T. Detection of malaria parasites in thick blood films. 2011 Annual
624 International Conference of the IEEE Engineering in Medicine and Biology Society, 2011, pp. 5140–5144.
- 625 23. Ghosh, M.; Das, D.; Chakraborty, C.; Ray, A. Plasmodium vivax segmentation using modified fuzzy
626 divergence. 2011 International Conference on Image Information Processing, 2011, pp. 1–5.
- 627 24. Di Ruberto, C.; Putzu, L. Accurate blood cells segmentation through intuitionistic fuzzy set threshold.
628 Proceedings of the 2014 International Conference on Signal Image Technology and Internet based Systems
629 (SITIS), 2014, pp. 57–64.
- 630 25. Kareem, S.; Morling, R.; Kale, I. A novel method to count the red blood cells in thin blood films. Proceedings
631 of 2011 IEEE International Symposium on Circuits and Systems (ISCAS), 2011, pp. 1021–1024.
- 632 26. Mushabe, M.; Dendere, R.; Douglas, T. Automated detection of malaria in Giemsa-stained thin blood
633 smears. 2013 35th Annual International Conference of the IEEE Engineering in Medicine and Biology
634 Society (EMBC), 2013, pp. 3698–3701.
- 635 27. Ross, N.; Pritchard, C.; Rubin, D.; Dusé, A. Automated image processing method for the diagnosis and
636 classification of malaria on thin blood smears. *Medical and Biological Engineering and Computing* **2006**,
637 *44*, 427–436.
- 638 28. Savkare, S.; Narote, S. Automatic detection of malaria parasites for estimating parasitemia. *International
639 Journal of Computer Science and Security (IJCSS)* **2011**, *5*, 310–315.
- 640 29. Otsu, N. A threshold selection method from gray-level histograms. *Automatica* **1975**, *11*, 23–27.
- 641 30. Somasekar, J.; Reddy, B. A Novel Two-Stage Thresholding Method for Segmentation of Malaria Parasites
642 in Microscopic Blood Images. *Journal of Biomedical Engineering and Medical Imaging* **2017**, *4*, 31–42.

- 643 31. Ahirwar, N.; Pattnaik, S.; Acharya, B. Advanced image analysis based system for automatic detection
644 and classification of malarial parasite in blood images. *International Journal of Information Technology and*
645 *Knowledge Management* **2012**, *5*, 59–64.
- 646 32. Khan, M.; Acharya, B.; Singh, B.; Soni, J. Content based image retrieval approaches for detection of malarial
647 parasite in blood images. *International Journal of Biometrics and Bioinformatics (IJBB)* **2011**, *5*, 97.
- 648 33. Rosado, L.; da Costa, J.C.; Elias, D.; Cardoso, J. Mobile-Based Analysis of Malaria-Infected Thin Blood
649 Smears: Automated Species and Life Cycle Stage Determination. *Sensors* **2017**, *17*, 1–22.
- 650 34. Soni, J.; Mishra, N.; Kamargaonkar, C. Automatic difference between RBC and Malaria parasites based on
651 morphology with frst order features using image processing. *Int. J. Adv. Eng. Technol* **2011**, *1*, 290–297.
- 652 35. Yunda, L.; Alarcón, A.; Millán, J. Automated image analysis method for p-vivax malaria parasite detection
653 in thick film blood images. *Sistemas & Telemática* **2012**, *10*, 9–25.
- 654 36. Das, D.; Ghosh, M.; Chakraborty, C.; Maiti, A.; Pal, M. Probabilistic prediction of malaria using
655 morphological and textural information. *Image Information Processing (ICIIP)*, 2011 International
656 Conference on, 2011, pp. 1–6.
- 657 37. Das, D.; Ghosh, M.; Pal, M.; Maiti, A.; Chakraborty, C. Machine learning approach for automated screening
658 of malaria parasite using light microscopic images. *Micron* **2013**, *45*, 97 – 106.
- 659 38. Das, D.; Maiti, A.; Chakraborty, C. Textural pattern classification of microscopic images for malaria
660 screening. *Advances in Therapeutic Engineering* **2014**, pp. 419–446.
- 661 39. Devi, S.; Singha, J.; Sharma, M.; Laskar, R. Erythrocyte segmentation for quantification in microscopic
662 images of thin blood smears. *Journal of Intelligent and Fuzzy Systems* **2017**, *32*, 2847–2856.
- 663 40. Dey, R.; Roy, K.; Bhattacharjee, D.; Nasipuri, M.; Ghosh, P. An Automated system for Segmenting platelets
664 from Microscopic images of Blood Cells. Proceedings of the 2015 International Symposium on Advanced
665 Computing and Communication (ISACC), 2015, pp. 230–237.
- 666 41. Diaz, G.; Gonzalez, F.; Romero, E. A semi-automatic method for quantification and classification of
667 erythrocytes infected with malaria parasites in microscopic images. *Journal of Biomedical Informatics* **2009**,
668 *42*, 296–307.
- 669 42. Savkare, S.; Narote, S. Blood Cell Segmentation from Microscopic Blood Images. Proceedings of the 2015
670 International Conference on Information Processing (ICIP), 2015, pp. 502–505.
- 671 43. Savkare, S.; Narote, S. Automatic Classification of Normal and Infected Blood Cells for Parasitemia
672 Detection. *International Journal of Computer Science and Network Security (IJCSS)* **2011**, *11*, 94–97.
- 673 44. Špringl, V. Automatic malaria diagnosis through microscopy imaging. *FACULTY OF ELECTRICAL
674 ENGINEERING* **2009**, p. 128.
- 675 45. Sulistyawati, D.; Rahmanti, F.; Purnama, I.; Purnomo, M. Automatic Segmentation of Malaria Parasites
676 on Thick Blood Film using Blob Analysis. Proceedings of the 2015 International Seminar on Intelligent
677 Technology and Its Applications, 2015, pp. 137–142.
- 678 46. Tek, F.; Dempster, A.; Kale, I. Malaria parasite detection in peripheral blood images. Proceedings of the
679 British Machine Vision Conference 2006 - BMVC 2006, 2006, pp. 347–356.
- 680 47. Jiang, X. Feature extraction for image recognition and computer vision. Proceedings - 2009 2nd IEEE
681 International Conference on Computer Science and Information Technology, ICCSIT 2009, 2009, pp. 1–15.
- 682 48. Malihi, L.; Ansari-Asl, K.; Behbahani, A. Malaria parasite detection in giemsa-stained blood cell images.
683 2013 8th Iranian Conference on Machine Vision and Image Processing (MVIP), 2013, pp. 360–365.
- 684 49. Kaur, B.; Kaur, S.P. Applications of Mathematical Morphology in Image Processing: A Review 1 **2013**.
- 685 50. Chen, S.; Zhao, M.; Wu, G.; Yao, C.; Zhang, J. Recent advances in morphological cell image analysis.
686 *Computational and Mathematical Methods in Medicine* **2012**, 2012.
- 687 51. M.A., S. Biomedical Image Processing with Morphology-Based Nonlinear Filters. *Ph.D Dissertation,
688 University of Texas at Austin* **1994**.
- 689 52. Rosado, L.; da Costa, J.M.C.; Elias, D.; Cardoso, J.S. A review of automatic malaria parasites detection and
690 segmentation in microscopic images. *Anti-Infective Agents* **2016**.